

Table of contents:

Supplemental Figures

Figure S1: Scheme of metabolic signaling pathways and outcomes.	S2
Figure S2: Aspart and pramlintide secondary structure remains unchanged by CB[7]-PEG.	S3
Figure S3: ¹ H NMR demonstrating Insulin/CB[7]-PEG binding.	S4
Figure S4: ¹ H NMR titration demonstrating Insulin/CB[7]-PEG binding.	S4
Figure S5: Novolog and Humalog are stabilized by CB[7]-PEG.	S5
Figure S6: Blood glucose following a meal in diabetic pigs.	S8
Figure S7: Zinc-free lispro-pramlintide co-formulation is stabilized by lower concentrations of CB[7]-PEG.	S10
Figure S8: Liver and kidney histopathology and function are unchanged after 6 weeks of daily dosing with CB[7]-PEG.	S12
Figure S9: Liver and kidney blood chemistry after intermittent dosing with CB[7]-PEG insulin-pramlintide co-formulation in diabetic pigs.	S13

Supplemental Results & Discussion

Circular dichroism of protein complexes with CB[7]-PEG	S3
In vitro stability	S5
Pramlintide ratio rationale	S5
Insulin pharmacokinetics - area under the curve	S7
Animal model advantages and limitations	S7
Biocompatibility	S11
<u>References</u>	S16

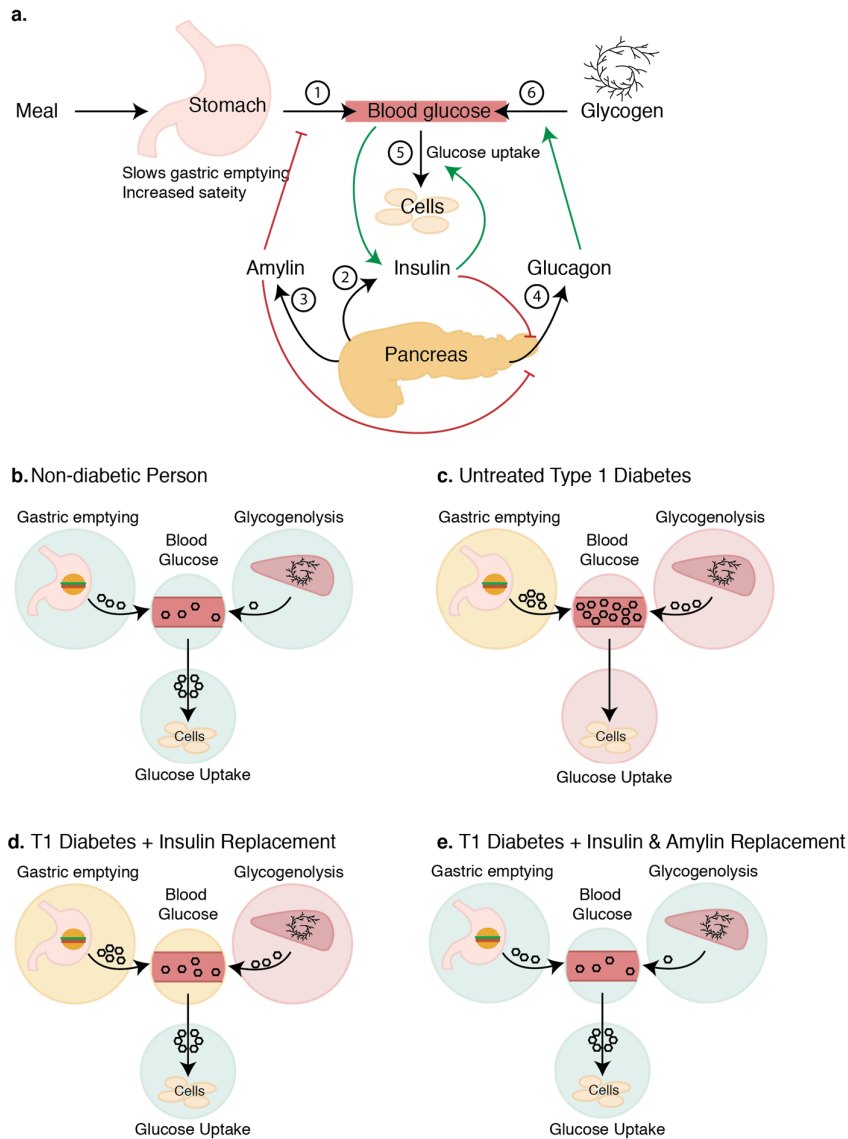


Figure S1: Scheme of metabolic signaling pathways and outcomes. **a**, Scheme of post-meal metabolic signaling pathways in a healthy human: (1) after a meal, gastric emptying results in increased blood glucose; (2) Insulin is secreted from the beta-cells in the pancreas in response to increased blood glucose levels and local signaling also results in glucagon suppression; (3) Amylin is secreted alongside insulin from the pancreatic beta-cells and inhibits gastric emptying and glucagon secretion by pancreatic alpha-cells; (4) Glucagon release from pancreatic alpha cells (suppressed by insulin and amylin); (5) Cellular glucose uptake is promoted by insulin, which results in blood glucose homeostasis; (6) Gluconeogenesis of liver glycogen stores is promoted by glucagon to release glucose into the blood (down-regulated by insulin and pramlintide mediated glucagon suppression). Summary of treatment outcomes on blood glucose, gastric emptying, glycogenolysis and gluconeogenesis, and cellular glucose uptake in **b**, healthy person, **c**, untreated type 1 diabetes, **d**, type 1 diabetes treated with insulin, **e**, type 1 diabetes treated with insulin and amylin. While exogenous insulin replacement therapy restores cellular glucose uptake, it alone cannot restore glucagon suppression or slow gastric emptying, which often results in poor blood glucose control. Amylin replacement therapy is critical to restore glucagon suppression and mimic endogenous metabolic signaling.

Circular dichroism of protein complexes with CB[7]-PEG

To confirm that CB[7]-PEG binding did not change the secondary structure of insulin aspart or pramlintide, we used circular dichroism to characterize their secondary structures when bound to CB[7]-PEG (Figure S2). Aspart was formulated with CB[7]-PEG (0.2 mM) to ensure that greater than 95% of the protein would be complexed. CB[7]-PEG did not alter the secondary structure of either aspart or pramlintide in formulation, whether in the presence or absence of EDTA to sequester formulation zinc (Figure S2). Under the same formulation conditions, pramlintide was approximately 80% bound and no difference in protein secondary structure was observed. From these studies we concluded that formulation with CB[7]-PEG does not significantly alter the structure of insulin and pramlintide.

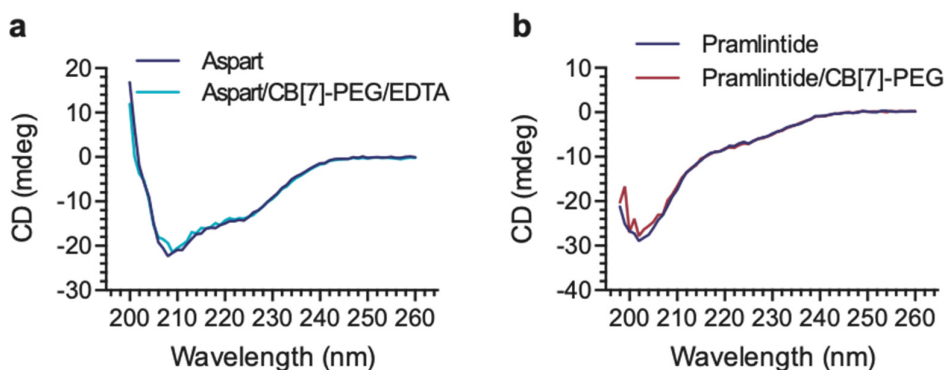


Figure S2: Aspart and pramlintide secondary structure remains unchanged by CB[7]-PEG. Circular dichroism spectra from 200-260nm for **a**, aspart and **b**, pramlintide. In these experiments, commercial Novolog was diluted to 0.2mg/mL in PBS and was evaluated alone, and with both EDTA (1:1 molar ratio to zinc) and CB[7]-PEG (5:1 molar excess to insulin). Pramlintide (PBS; pH~7.4; 0.5 mg/mL) was evaluated alone and with CB[7]-PEG (1.1 mg/mL). Data shown is n=1 independent experiment.

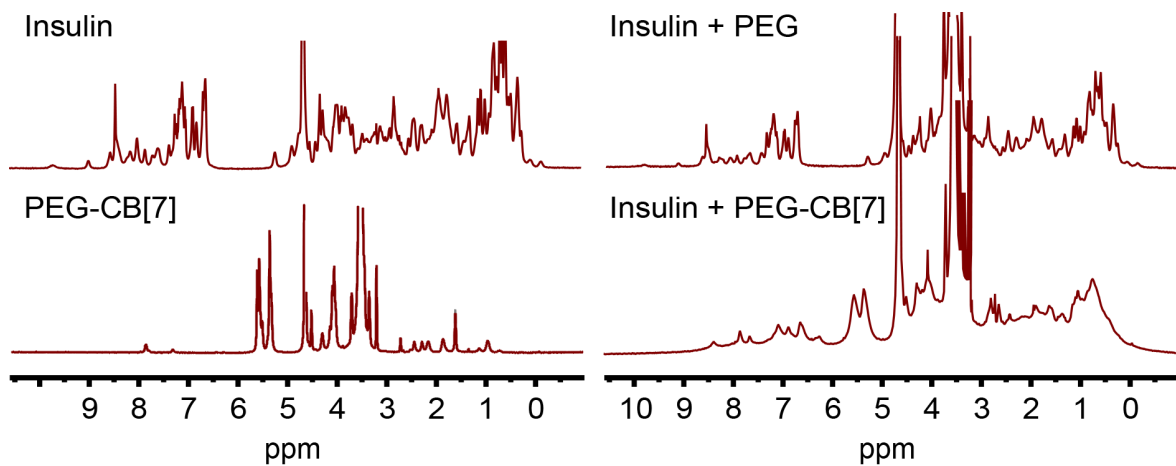


Figure S3: ¹H NMR demonstrating Insulin/CB[7]-PEG binding. Groups include: (i) insulin, (ii) insulin and free PEG_{5k}, (iii) CB[7]-PEG and (iv) insulin/CB[7]-PEG complex. Experiments were performed once (n=1 sample).

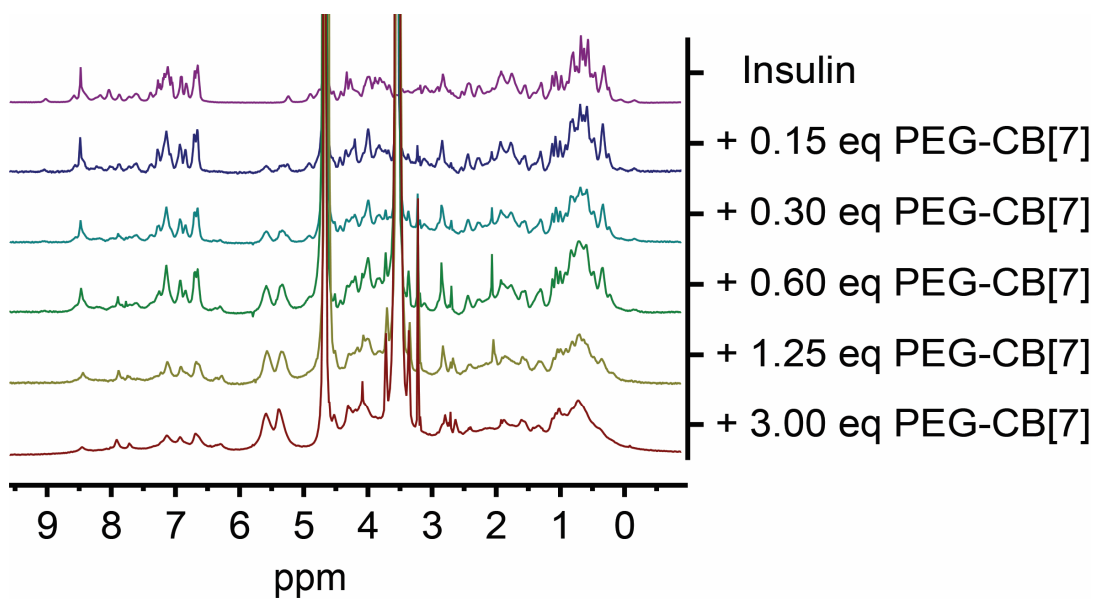


Figure S4: ¹H NMR titration demonstrating Insulin/CB[7]-PEG binding. Insulin/CB[7]-PEG complex can be tracked by the emergence of the characteristic peak ~6.4 ppm. Broadening of all signals was observed in the complex, likely due to short T₂ relaxation caused by quick exchange of CB[7]-PEG. Experiments were performed once (n=1 sample).

***In vitro* stability**

In these assays, commercial Novolog aggregated in 10 ± 1.0 hrs under stressed conditions while zinc-free Novolog formulations (created using a 1:1 molar ratio of EDTA to zinc) were significantly less stable and aggregated following only 3.2 ± 0.2 hrs. Humalog showed higher stability, but similar trends with commercial Humalog aggregating after 48 ± 18 hrs (n=3) and zinc-free Humalog aggregating after 16 ± 7 hrs. These observations suggest that removal of formulation zinc destabilizes the insulin hexamer and encourages insulin aggregation, consistent with previous work. In contrast, zinc-free aspart/CB[7]-PEG and zinc-free lispro/CB[7]-PEG formulations did not aggregate during the entire 100-hour kinetic study (Figure 2, Figure S3).

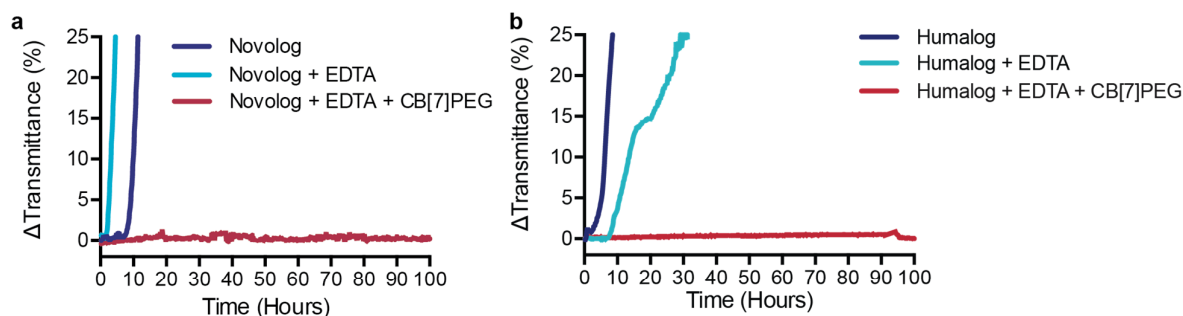


Figure S5: Novolog and Humalog are stabilized by CB[7]-PEG. *In vitro* stability of **a**, Novolog, zinc-free Novolog (with EDTA as a chelator), and zinc-free Novolog formulated with CB[7]-PEG and **b**, Humalog, zinc-free Humalog (with EDTA as a chelator), and zinc-free Humalog formulated with CB[7]-PEG. Kinetic profiling of the aggregation of insulin formulations using change in transmittance at 540nm. Experiments were conducted at pH~7.4, 37°C, in physiological buffer with continuous agitation over the course of 100 h, demonstrating that formulation with CB[7]-PEG resists aggregation over the period assayed. Data shown are the average transmittance trace for n = 3 samples per group.

Pramlintide ratio rationale

The fixed molar ratios of endogenous amylin to insulin reported in the literature range from 1:20 and 1:7.^[1-3] *In silico* experiments have indicated that an insulin:pramlintide ratio greater than 1:8 may be most effective, specifically in the range of 1:4-1:2.^[4] In initial blood glucose studies in rats, each treatment group was evaluated at different molar ratios of pramlintide to insulin of 1:15, 1:8, or 1:2. Pramlintide:insulin molar ratios of 1:15 and 1:8 are representative of endogenous amylin:insulin secretion, and a 1:2 formulation was also evaluated to

increase the signal-to-noise ratio for *in vivo* pharmacokinetic studies. No difference in blood glucose response was observed between the various pramlintide concentrations evaluated. In diabetic rats, a pramlintide:insulin molar ratio of 1:2 was necessary for reliable determination of pharmacokinetics by ELISA. As pigs are larger and dosing is more similar to human, it was possible to evaluate systemic concentrations at lower pramlintide doses. Thus, pramlintide was formulated at a molar ratio of 1:6 pramlintide:insulin. This dose was similar to reported endogenous values and above the 1:8 ratio predicted by *in silico* experiments. A lower pramlintide dose was chosen as clinical studies indicate that higher doses of pramlintide are often associated with increased gastrointestinal side effects and discontinuation of use.^[5] In the pig studies, a 1:6 pramlintide:insulin (4U insulin) dose was equivalent to administration of a 15µg dose of pramlintide, which is consistent with the starting dose for patients with Type 1 diabetes using Symlin.

To facilitate future clinical translation to human patients, further study will be required to optimize the effective fixed dose of the two hormones for treatment of diabetes. Recent work by Riddle reports the evaluation of fixed-dose pramlintide:insulin ratios of 1:4, 1:2.5, and 1:2 as treatments for diabetes and all ratios were found to suppress post-prandial glucagon.^[6] There is currently non consensus regarding the optimal pramlintide:insulin ratio, which is nonetheless likely to also be highly dependent on the specific formulation used. We believe the “best” pramlintide:insulin ratio to optimize insulin function will contain the lowest pramlintide dose that results in delayed gastric emptying and sufficient post-prandial glucagon suppression in humans. As mentioned above, many of the negative side effects of pramlintide observed clinically occur at higher doses.^[5] Based on the post-prandial glucagon suppression data we report for diabetic pigs, we believe that one of the advantages of our insulin/pramlintide co-formulation is that synergistic pramlintide action may be observed at lower doses than is possible when insulin and pramlintide are delivered separately.

Insulin pharmacokinetics - area under the curve

In pharmacokinetic experiments in both rats and pigs, insulin-pramlintide co-formulations demonstrate decreased peak insulin serum concentrations and decreased AUC over 60 minutes compared to commercial Novolog or Humalog administered alone (in rat experiments $p=0.001$; in pig experiments $p=0.081$), and to separate injections of Novolog or Humalog and pramlintide (in rat experiments $p=0.052$; in pig experiments $p=0.017$). Previous studies have linked insulin-pramlintide dual-hormone treatment to increased insulin sensitivity and lower serum insulin levels.^[7] Indeed, it is recommended that insulin doses are reduced by 50% when administering pramlintide in meal-time treatments to prevent hypoglycaemia.^[8] While it has been observed that individuals with high insulin sensitivity have a higher rate of insulin clearance from the blood stream,^[9] the exact mechanism relating insulin sensitivity and insulin clearance is unknown at present.^[9] Increased insulin sensitivity may explain the decrease in insulin serum concentrations observed in animals receiving insulin-pramlintide co-formulations, where the two therapeutic proteins have much more similar pharmacokinetics when compared to controls, and thus greater potential for synergistic action. Future investigation of the dose-dependent effects of co-formulated pramlintide on insulin sensitivity and clearance may have powerful clinical implications in reducing the risk of hyperinsulinemia in diabetic patients.

Animal model advantages and limitations

In vivo diabetic rat model

Rats were an ideal first model to test novel insulin formulations. Our intention in conducting these rat studies was to determine the potential for our approach to co-formulation of

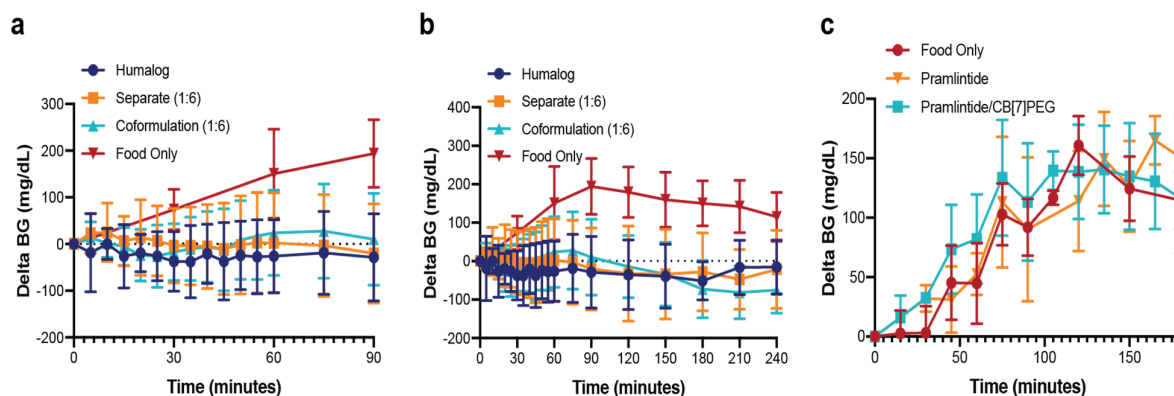


Figure S6: Blood glucose following a meal in diabetic pigs. *a/b*, diabetic pigs received subcutaneous administration of either (i) commercial Humalog (n=15), (ii) commercial Humalog and pramlintide (pH=4) delivered in separate injections (n=15), (iii) lispro-pramlintide co-formulation with CB[7]-PEG (n=15), or (iv) no treatment (n=6). Treatments were administered simultaneously with a 200g meal. All treatment groups received 4U insulin and pramlintide groups received a molar ratio of 1:6 of pramlintide:lispro. *c*, a gastric emptying study was performed to assess blood glucose levels after a meal without treatment with insulin. Diabetic pigs received either (i) no treatment (n=6), (ii) pramlintide (pH=4) (n=5), or (iii) pramlintide formulated with CB[7]-PEG (n=5). Pramlintide treatments were administered at a dose equivalent to the a pramlintide:insulin ratio of 1:6 with a 4U insulin dose. Blood glucose was measured using handheld glucose monitors. Error bars, mean \pm s.d.

pramlintide and insulin using non-covalent PEGylation to modify pramlintide

pharmacokinetics before progressing into large animal studies. STZ induced type-1 like

models of diabetes are well established in rats. Unlike mice who experience stress-related

glucose spikes, rats can be trained to receive subcutaneous injections and will co-operate

for blood collection while conscious without experiencing stress. Rats are also large enough

that frequent blood collection is possible to obtain high resolution pharmacokinetic data.

Unfortunately, rats graze on food constantly during their waking hours and assessment of

drug action during a discrete meal is extremely difficult to impossible. Therefore, it was not

possible to conduct treatment efficacy tests in rats as the primary modes of action of

pramlintide include slowing gastric emptying and increasing satiety at meal-times, both of

which slow the introduction of glucose into the blood. As such, we expected there to be a

negligible effect in blood glucose depletion between formulations when using fasted rats

according to the standard protocols used in these studies. Nevertheless, these studies in

fasted rats allowed us to evaluate the pharmacokinetic characteristics of insulin and

pramlintide when dosed together in our co-formulation in comparison to the clinical standard of dosing pramlintide and insulin separately.

In vivo diabetic pig model

After initial proof-of-concept in a rat model, a large animal model was necessary to address some of the limitations in the rat model. Rodents have loose skin, allowing for much more rapid uptake of compounds administered subcutaneously. In contrast, pigs have skin that is closely reminiscent of human skin and thus exhibit many similarities with regard to pharmacokinetics of compounds following subcutaneous administration and the overall metabolic behavior of the two species.^[10] The larger size of the pigs also allows for the delivery of neat commercial insulin (100U/mL), which is important to preserve the solution equilibrium of insulin multimers to more accurately assess pharmacokinetics. Moreover, pigs can be fed discrete meals, which allowed us to probe the efficacy of our co-formulation in preventing post-prandial glucagon mobilization. Unfortunately, the diabetic pig model was unable to capture the delayed gastric emptying effects of pramlintide at mealtimes, likely on account of the pig chow used in accordance with IACUC regulation. Control experiments were conducted by dosing high concentrations of pramlintide alone, or pramlintide formulated with CB[7]-PEG, and no difference in blood glucose increases following a meal were observed compared to the control groups receiving no treatment (Figure S4c). It has been reported that the fibre, fat, and protein content in meals can act to naturally slow gastric emptying.^[11-14] Unlike most human diets, the pig chow given to the diabetic pigs at mealtimes in these studies is highly balanced and high in fibre (Teklad Miniswine Diet 8753). One unfortunate side-effect of this observation is that the impact of pramlintide on gastric emptying in these diabetic pigs is likely masked by already significantly delayed gastric emptying profiles expected from the pig chow used in these studies.

Formulation pharmacokinetics in rat and pig models

Previous studies in rodent models of insulin-deficient diabetes have observed a consistent time-to-peak onset between rapid-acting insulin analogues and regular insulin.^[15] This contrasts with human studies in which “rapid-acting” insulin formulations exhibit time-to-onset that is reduced roughly by half.^[16] The difference between the pharmacokinetics observed in rats and humans (or pigs) arises on account of two important differences in the animal models: (i) the dilution of the formulations required to enable accurate dosing in rats, and (ii) differences in absorption from the s.c. space arising from physiological differences between these species. First, the size of the rat necessitates dilution of insulin formulations to facilitate administration of an accurate dose. Dilution of insulin shifts the equilibrium of the insulin association states and favors the monomeric and dimeric forms of the insulin instead of the hexameric form. In contrast, pramlintide only exists in a monomeric form and is unaffected by the dilution. Secondly, rats have loose skin that facilitates more rapid absorption of administered compounds following s.c. administration on account of the greater surface area available for absorption.

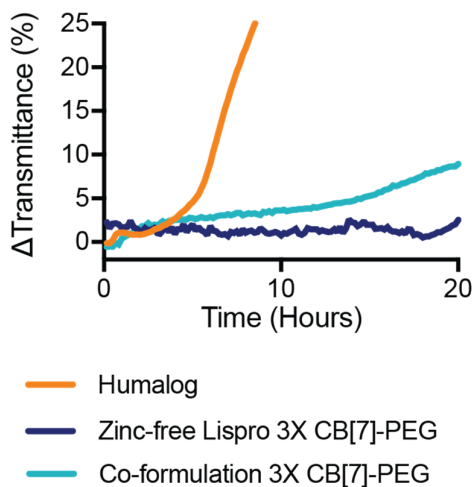


Figure S7: Zinc-free lispro-pramlintide co-formulation is stabilized by lower concentrations of CB[7]-PEG. *In vitro* stability of zinc-free lispro formulated with CB[7]-PEG (molar ratio of 3:1 CB[7]-PEG:lispro), was compared with zinc-free lispro-pramlintide co-formulation with CB[7]-PEG (molar ratio of 3:1 CB[7]-PEG:lispro+pramlintide). Both formulations were more stable than commercial Humalog alone. Kinetic profiling of the aggregation of insulin formulations using change in transmittance at 540nm. Experiments were conducted at pH~7.4, 37°C, in physiological buffer with continuous agitation over the course of 20 h, demonstrating that formulation with CB[7]-PEG resists aggregation longer than current commercial formulations over the period assayed. Data shown are the average transmittance trace for n = 3 samples per group.

In contrast, pigs are sufficiently large for insulin to be administered accurately using standard concentrations (100U/mL), ensuring the observed pharmacokinetics are not skewed by dilution effects. Pigs also have tight skin and subcutaneous tissue that is very similar to humans, making them the most relevant preclinical model for studying pharmacokinetics of biopharmaceuticals following subcutaneous administration. Indeed, the pharmacokinetics of pramlintide we observed in pigs are very similar to those reported in humans.^[8] Yet, insulin exhibits shorter duration of action in pigs than is typically observed in humans (2 hours in pigs vs. 4 hours in humans).^[10, 17, 18] It is possible that subcutaneous compartmental structure allows for greater formulation dilution upon injection, and thus more rapid insulin dissociation and absorption, than is observed in humans. More rapid absorption in pigs and rats may account for the similar insulin pharmacokinetics observed in our studies between commercial rapid-acting insulin analogues, administration of insulin and pramlintide in separate injections, or a single administration of insulin-pramlintide co-formulation.

Biocompatibility studies

As CB[7]-PEG is a new chemical entity, we sought to assess its biocompatibility by using blood chemistry and histopathology to look for negative effects on the liver or kidney. Healthy Sprague Dawley rats (n=4) received daily injections of CB[7]-PEG (at a dose equivalent to what would be administered in an insulin injection) for six weeks. Blood was collected on alternate weeks to assess blood chemistry for markers of liver and kidney failure (Figure S5). A control group of healthy rats housed under the same conditions, but who received no injections, were used to control for the impact of aging on blood chemistry values. Blood chemistry for both treatment and control groups were compared to a healthy population of Sprague Dawley rats (Age 8-9 weeks). Liver toxicity was assessed through measurement of alanine aminotransferase (ALT), aspartate aminotransferase (AST), alkaline phosphatase (ALP), and bilirubin. Kidney toxicity was evaluated by examining creatinine and blood urea nitrogen (BUN) levels. Values for ALT, AST, ALP, creatine, and

BUN were within the range of healthy rats (defined as the mean \pm 2 standard deviations) for both the treatment and control groups. ALP values for both control and treatment groups appear to decrease with age, which is consistent with observations in the literature.^[19, 20]

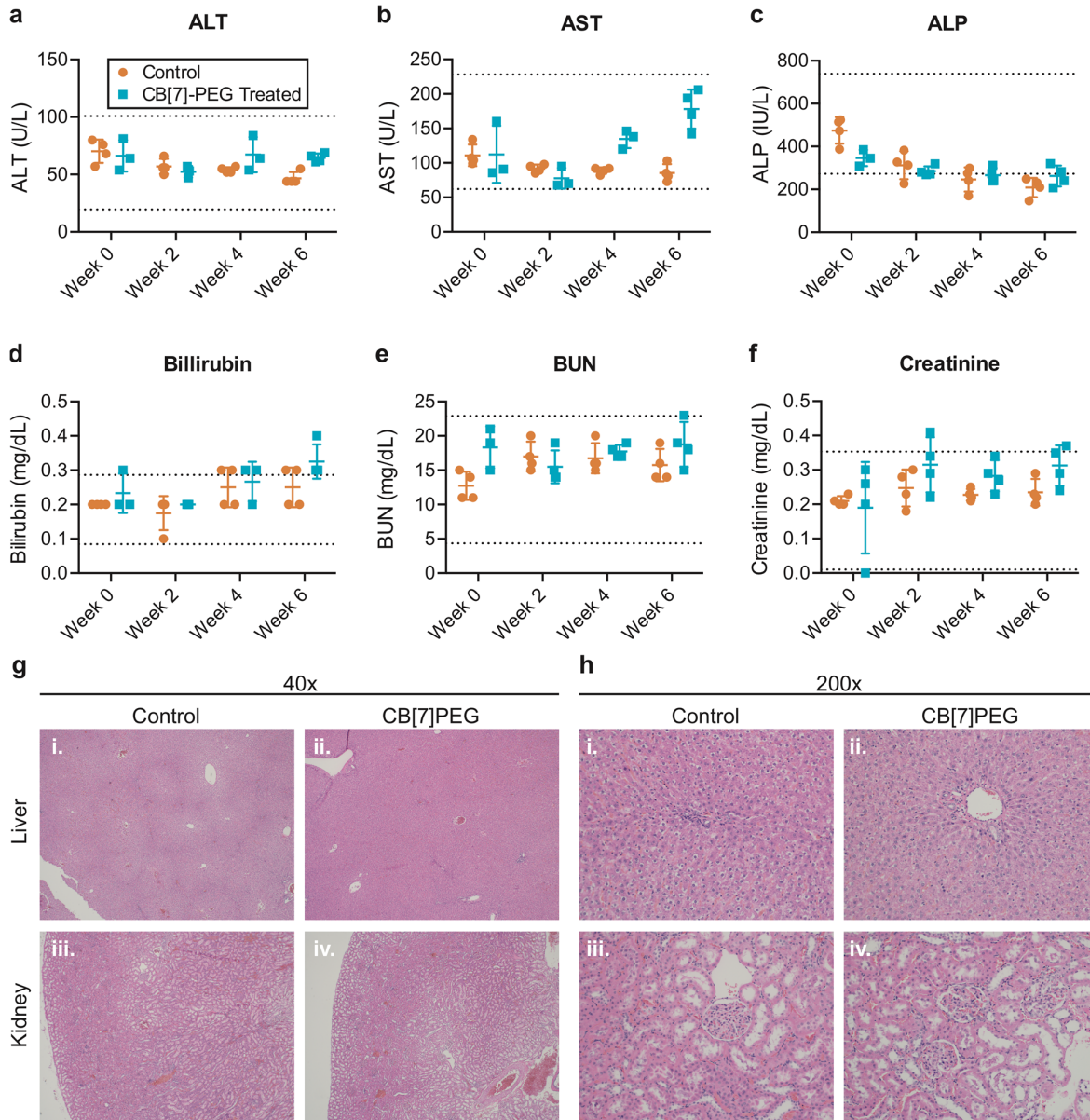


Figure S8: Liver and kidney histopathology and function are unchanged after 6 weeks of daily dosing with CB[7]-PEG. CB[7]-PEG (0.2mg/kg) was given daily via subcutaneous injection to healthy rats for 6 weeks to assess long-term liver and kidney toxicity of CB[7]-PEG under conditions mimicking daily therapeutic injections (n=4 animals for each group). **a-f**, Blood chemistry panels were performed biweekly throughout the treatment and blood chemistry markers stayed within a normal range throughout the treatment period. The dotted lines in each plot indicate the range of values exhibited in a healthy population of Sprague Dawley rats (Age 8-9 weeks), defined as the mean \pm two standard deviations. Error bars, mean \pm s.d. **g-h**, Histology sections from liver and kidney tissues after the treatment period were stained with H&E and show the tissues remained completely healthy. **g**, Histology sections taken at 40x magnification and **h**, sections taken at 200x magnification. For histology, the control was taken from n=1 rat. The treated samples are representative sections from n=4 rats.

Bilirubin values increased over the course of the study, though remained well within the range of normal bilirubin values for male Sprague Dawley rats reported by Charles River Laboratories to be between 0.1-1.0mg/dL.^[21]

A single-blind assessment of liver and kidney histology sections from treated and control rats was performed by a pathologist at the endpoint of the study. Haematoxylin and Eosin (H&E) and Masson's Trichrome staining were performed and no differences in fat content or fibrosis between the treated and untreated rats was observed in either tissue (Figure S5g-h). Liver portal triads in both control and treated samples appeared normal with no fibrosis. Some focal fat was observed in both treated and control tissues. There was no fibrosis observed in either treated or healthy kidney samples.

Evaluation of blood chemistry in diabetic pigs after repeated treatment with CB[7]-PEG during the course of the study corroborated the observations made in rats (Figure S6). Pigs were dosed with the insulin-pramlintide co-formulation containing CB[7]-PEG at 10-13 meals

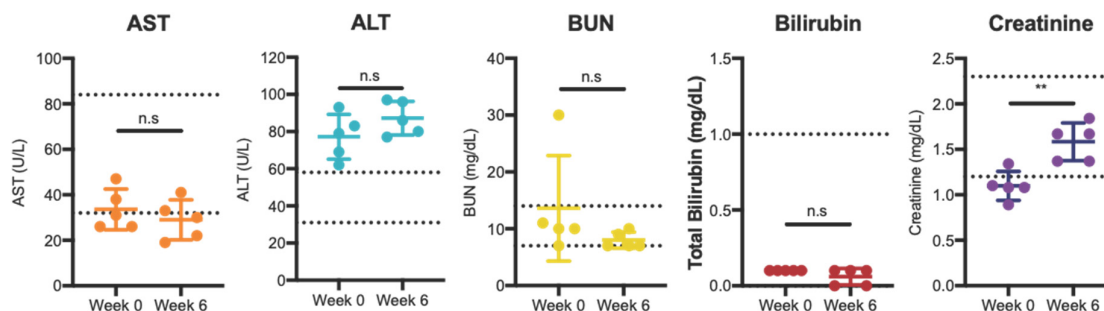


Figure S9: Liver and kidney blood chemistry after intermittent dosing with CB[7]-PEG insulin-pramlintide co-formulation in diabetic pigs. Diabetic pigs were dosed subcutaneously with the insulin-pramlintide co-formulation (1:6) containing CB[7]-PEG at 10-13 meals over the course of six weeks. Blood chemistry panels were performed at Week 0 using blood taken 3-4 days following the induction of diabetes, and Week 6 measurements were taken at the end of the study. The dotted lines in each plot indicate the range of values observed in treated animals is within the normal range for healthy pigs. It is important to note that diabetes induction with streptozotocin can cause liver and kidney damage that results in blood chemistry values that deviate outside the normal range. Here a two-tailed student's t test is used to evaluate statistical significance between time points. The only marker that demonstrates a statistically significant difference from the beginning to end of the study is creatinine ($p=0.001$); however, the Week 6 measurements fall well within the normal range. For all groups $n=5$ pigs. Error bars, mean \pm s.d.

over the course of six weeks. Week 0 measurements were taken 3-4 days following the induction of diabetes, and Week 6 measurements were taken at the end of the study.

CB[7] and PEG each have favorable toxicity profiles;^[22-27] free CB[7] administered i.v. in mice showed no toxicity up to doses of 200 mg/kg,^[28] while PEG has very low toxicity and 10 mg/kg is considered acceptable daily intake.^[29] Literature reports of CB[7] highlight that while the molecule may be taken up into cells, no toxic effects are observed.^[26, 30] While CB[7] can bind very strongly to numerous guests, extensive review of the literature suggests that CB[7] does not bind to lipids found in mammalian cell membranes.^[31] It was therefore expected that conjugated CB[7]-PEG would be similarly benign. The dose of CB[7]-PEG delivered in our insulin-pramlintide formulations in rats is 0.2 mg/kg, which is several orders of magnitude below the maximum tolerated dose of either CB[7] or PEG alone. As expected, no significant toxic effects were observed after six weeks of daily treatment with CB[7]-PEG. No previous studies have been published assessing the organ toxicity of CB[7] in mammals. In addition, both CB[7] and PEG have been investigated individually^[22, 25] and have been shown to be cleared rapidly through the kidneys without any observable accumulation in tissues. Since the hydrodynamic size of CB[7]-PEG (MW~6.2 kDa) is similar to PEG alone (MW~5 kDa), CB[7]-PEG falls well below the molecular weight cutoff typically observed for renal clearance. For this reason, we expect that the compound will be cleared similarly to either component alone. In these studies, we did not observe in single-blinded histopathology any signs of liver or kidney toxicity after six weeks of daily treatment of CB[7]-PEG. Further biocompatibility studies will be needed to assess whether CB[7]-PEG has long term health effects, but the results shown here suggest that CB[7]-PEG is well-tolerated.

Future studies will also require comprehensive immunogenicity studies of the complete insulin pramlintide co-formulation with CB[7]-PEG. The high degree of stability of our co-formulation should be advantageous with respect to immunogenicity, which is often observed to arise on account of the presence of protein aggregates in formulation.^[32, 33]

References

1. Sanke, T. *et al.* Plasma islet amyloid polypeptide (Amylin) levels and their responses to oral glucose in type 2 (non-insulin-dependent) diabetic patients. *Diabetologia*. **34**, 129-132 (1991).
2. Martin, C. The physiology of amylin and insulin: maintaining the balance between glucose secretion and glucose uptake. *Diabetes Educator*. **32**, 101S-104S (2006).
3. Hay, D.L. *et al.* Amylin: pharmacology, physiology, and clinical potential. *Pharmacol. Rev.* **67**, 564 (2015).
4. Micheletto, F. *et al.* In silico design of optimal ratio for co-administration of pramlintide and insulin in type 1 diabetes. *Diabetes Technol. The.* **15**, 802-809 (2013).
5. Kolterman, O.G. *et al.* Effect of 14 days' subcutaneous administration of the human amylin analogue, pramlintide (AC137), on an intravenous insulin challenge and response to a standard liquid meal in patients with IDDM. *Diabetologia*. **39**, 492-499 (1996).
6. Riddle, M.C., *et al.* Fixed ratio dosing of pramlintide with regular insulin before a standard meal in patients with type 1 diabetes. *Diabetes Obes. Metab.* **17**, 904-907 (2015).
7. Hinshaw, L. *et al.* Effects of delayed gastric emptying on postprandial glucose kinetics, insulin sensitivity, and β -cell function. *Am. J. Physiol-Endoc. M.* **307**, E494-E502 (2014).
8. Astrazeneca Pharmaceuticals, L.P. *SYMLIN (pramlintide acetate) injection*. FDA. (2014).
9. Ahrén, B. & Thorsson, O. Increased insulin sensitivity is associated with reduced insulin and glucagon secretion and increased insulin clearance in man. *J. Clin. Endocr. Metab.* **88**, 1264-1270 (2003).
10. Larsen, M.O. & Rolin, B. Use of the Gottingen Minipig as a Model of Diabetes, with Special Focus on Type 1 Diabetes Research. *ILAR*. **45**, 303-313 (2004).
11. Benini, L., *et al.* Gastric emptying of a solid meal is accelerated by the removal of dietary fibre naturally present in food. *Gut*. **36**, 825-830 (1995).
12. Yu, K., *et al.* The impact of soluble dietary fibre on gastric emptying, postprandial blood glucose and insulin in patients with type 2 diabetes. *Asia Pac. J. Clin. Nutr.* **23**, 210-218 (2014).

13. Gentilcore, D., *et al.* Effects of Fat on Gastric Emptying of and the Glycemic, Insulin, and Incretin Responses to a Carbohydrate Meal in Type 2 Diabetes. *J. Clin. Endocr. Metab.* **91**, 2062-2067 (2006).
14. Ma, J., *et al.* Effects of a Protein Preload on Gastric Emptying, Glycemia, and Gut Hormones After a Carbohydrate Meal in Diet-Controlled Type 2 Diabetes. *Diabetes Care.* **32**, 1600 (2009).
15. Plum, A., Agersø, H. & Andersen, L. Pharmacokinetics of the rapid-acting insulin analog, insulin aspart, in rats, dogs, and pigs, and pharmacodynamics of insulin aspart in pigs. *Drug Metab. Dispos.* **28**, 155-160 (2000).
16. Heinemann, L., *et al.* Variability of the metabolic effect of soluble insulin and the rapid-acting insulin analog insulin aspart. *Diabetes Care.* **21**, 1910-1914 (1998).
17. Radziuk, J.M., *et al.* Bioavailability and bioeffectiveness of subcutaneous human insulin and two of its analogs--LysB28ProB29-human insulin and AspB10LysB28ProB29-human insulin--assessed in a conscious pig model. *Diabetes.* **46**, 548-556 (1997).
18. Kildegaard, J., *et al.* Elucidating the Mechanism of Absorption of Fast-Acting Insulin Aspart: The Role of Niacinamide. *Pharm. Res.* **36**, 49 (2019).
19. Wolford, S.T., *et al.* Age-related changes in serum chemistry and hematology values in normal Sprague-Dawley rats. *Fund. Appl. Toxicol.* **8**, 80-88 (1987).
20. Lillie, L.E., *et al.* Reference values for young normal Sprague-Dawley rats: weight gain, hematology and clinical chemistry. *Hum. Exp. Toxicol.* **15**, 612-616 (1996).
21. Giknis, M.L.A. and C.B. Clifford, Clinical Laboratory Parameters for Crl:CD (SD) Rats. Charles River Laboratories (2006).
22. Yin, H. & Wang, R. Applications of cucurbit[n]urils (n=7 or 8) in pharmaceutical sciences and complexation of biomolecules. *Isr. J. Chem.* **58**, 188-198 (2018).
23. Fruijtier-Pölloth, C. Safety assessment on polyethylene glycols (PEGs) and their derivatives as used in cosmetic products. *Toxicology.* **214**, 1-38 (2005).
24. Webster, R. *et al.* PEGylated proteins: evaluation of their safety in the absence of definitive metabolism studies. *Drug Metab. Dispos.* **35**, 9-16 (2007).

25. Webster, R., *et al.* "PEG and PEG Conjugates Toxicity: Towards an Understanding of the Toxicity of PEG and Its Relevance to PEGylated Biologicals." In *PEGylated Protein Drugs: Basic Science and Clinical Applications*, edited by F.M. Veronese, 127–146. Basel: Birkhäuser Basel (2009).
26. Hettiarachchi, G. *et al.* Toxicology and drug delivery by cucurbit[n]uril type molecular containers. *PLoS One*. **5**, e10514 (2010).
27. Kuok, K.I. *et al.* Cucurbit[7]uril: an emerging candidate for pharmaceutical excipients. *Ann. NY. Acad. Sci.* **1398**, 108-119 (2017).
28. Uzunova, V.D. *et al.* Toxicity of cucurbit[7]uril and cucurbit[8]uril: an exploratory in vitro and in vivo study. *Org. Biomol. Chem.* **8**, 2037-2042 (2010).
29. FAO/WHO. Evaluation of certain food additives. Twenty-third report of the joint FAO/WHO expert committee on food additives. *World Health Organ Tech. Rep. Ser. No.* **648**, (1980).
30. Walker, S., *et al.* The Potential of Cucurbit[n]urils in Drug Delivery. *Isr. J. Chem.* **51**, 616–24 (2011).
31. Barrow, S.J. *et al.* Cucurbituril-based molecular recognition. *Chem. Rev.* **115**, 12320-12406 (2015).
32. Fineberg, S.E., *et al.* Immunological Responses to Exogenous Insulin. *Endocr Rev.* **28**, 625-652 (2007).
33. Ratanji, K.D., *et al.* Immunogenicity of therapeutic proteins: influence of aggregation. *J. Immunotoxicol.* **11**, 99-109 (2014).